University of Tehran Press

DESERT

Online Issn: 475-2345X

Home page: https://jdesert.ut.ac.ir/

Detection of Vegetation Changes in Agricultural Lands of Sistan Plain using Remote Sensing Technique

Zohreh Mosleh Ghahfarokhi[1*], Mohsen Bagheri Bodaghabadi[2]

[1] Soil and Water Research Department, Chaharmahal and Bakhtiari Agricultural and Natural Resources Research and Education Center, Agricultural Research, Education and Extension Organization(AREEO), Shahrekord, Iran. Email: z.mosleh@areeo.ac.ir

[2] Soil and Water Research Institute (SWRI), Agricultural Research, Education and Extension Organization (AREEO), Karaj, Iran. Email: m.baghery@areeo.ac.ir

Article Info.

Article type:
Research Article

Article history:
Received: 24 Dec. 2022
Received in revised from: 15 Feb. 2023
Accepted: 21 March 2023
Published online: 27 June 2023

Keywords:
Vegetation indices,
Remote sensing,
Environmental monitoring,
Google earth engine,
Landsat image.

ABSTRACT

Information about the state of vegetation is very important for environmental planning, land preparation and achieving sustainable development. In this study normalized differential vegetation index (NDVI) values were calculated based on Landsat 8 satellite images in order to show temporal and spatial changes in the vegetation cover of agricultural lands in Sistan plain over ten years (2011 to 2020) using the Google Earth Engine platform. Additionally, the NDVI index were classified using decision tree algorithm in order to analyze vegetation changes using thematic change workflow method. By comparing classified images with reference samples which collected from ground sampling, validation was carried out. Then, in order to assess accuracy of vegetation maps, the error matrix was prepared, the overall accuracy and kappa indices were determined. The values of overall accuracy and kappa indices indicated optimal accuracy and it can be stated that there is moderate agreement between ground samples and the classified images (i.e., kappa index is 0.48 to 0.7). The central areas of Sistan plain have a decline in vegetation, whereas areas in northern and eastern have an increase. The cover vegetation on lands of Sistan plain decreased in 19260.4 ha while increased over 25633.2 ha throughout ten years. Examination of NDVI index shows instability of production in this area due to aforementioned factors.

Cite this article: Mosleh Ghahfarokhi, Z., Bagheri Bodaghabadi, M. (2023). Detection of Vegetation Changes in Agricultural Lands of Sistan Plain using Remote Sensing Technique. DESERT, 28 (1), DOI: 10.22059/jdesert.2023.93538

DOI: 10.22059/jdesert.2023.93538

Publisher: University of Tehran Press

1. Introduction

Vegetation cover change occurred over time and for a variety of reasons (human or natural) which has an impact on the ecosystem's conditions. Consequently, it is crucial to identify, anticipate, and keep track of such changes in ecosystems (Pettorelli et al., 2005). Planning and managing the environment require careful attention to vegetation cover change. The most crucial characteristics that enable the use of remote sensing information to inspect vegetation and regulate its changes preferable to alternative approaches are reproducibility, ease of access to information, high information accuracy, and cost and time savings. As a result, a lot of researchers have looked into vegetation using remote sensing data. In recent years, remote sensing specialists have used satellite data to monitor vegetation using vegetation indices, which have become widely employed. By using standard approaches, it is very difficult and expensive to gather data on vegetation changes. If using satellite data makes it possible to examine vegetation in great detail (Alavipanah, 2003).

In recent years, the use of remote sensing techniques has grown significantly in importance for identifying environmental changes, such as those in vegetation or urban areas (Lu et al., 2004; Rahman et al., 2019). Studies have demonstrated that using remote sensing techniques to study changes and create vegetation maps is quite effective (Alavipanah,et al., 2006; Alqurashi and Kumar, 2013; Braun et al., 2019; Kotaridis and Lazaridou, 2018). Plant indices and spectral ratio have been a topic of debate in scientific communities concerned with geographic information systems and remote sensing since the late 1970s. Since then, numerous indices have been developed to quantify and examine changes in vegetation over time, including NDVI, weighted difference vegetation index (WDVI), and soil adjusted vegetation index (SAVI). These indicators' foundation is based on the distinction between the red and near-infrared bands. Chlorophyll pigments selectively absorb blue (400–500 nm) and red (600–700 nm) wavelengths for photosynthesis. There is less absorption over the green wavelengths (500–600 nm) and thus the green appearance of healthy vegetation (Fatemi, 2012). Shafei and Hosseini (2012) using satellite data, examined the state of the vegetation in the Sistan region and assessed changes to the vegetation between 1990 and 2006. According to the findings, there was 26 thousand hectares of vegetation in 2006, down from 101 thousand hectares in 1990. Using the normalized index of vegetation cover difference, Mohammadyari et al. (2019) looked at the changes to the vegetation cover in the Karaj watershed in 2006, 2011 and 2017. According to the findings, 5104 ha (4%) increasing in vegetation has occurred on lands with very good vegetation cover. Also, the largest decrease in area is in lands with high coverage, which has decreased by 4055 ha (equivalent to 3%) in the studied period. They examined Landsat 5 and 8 and NDVI, MLC and CA-ANN indices for the years 1990, 2000, 2010 and 2020. The findings indicated that compared to the changes from 1990 to 2000, 2000 to 2010, and 1990 to 2020, those from 2010 to 2020 occurred far more quickly and with greater impressiveness. Therefore, agricultural land has grown by 3335 ha (or 34%) over this time.

Changes in plant cover are one of the most significant physical manifestations of land degradation in dry regions, according to many researchers (Verón et al., 2006; Reynolds et al., 2007). These changes are also currently one of the main indicators in the assessment of land degradation. Xie et al. (2019) evaluated the vegetation cover changes in rangelands from 1988 to 2017 using Landsat images and explained that vegetation cover decrease was observed in 20% of the study area. The lands with decrease in vegetation cover, covering a considerable area of 200000 km^2 which exhibited a markedly reduced resilience to droughts.

Today, despite the widespread use and free access to satellite images, receiving, storing and pre-processing of these images, take up most time of remote sensing projects. On the other hand, the need for computers with high memory usage and processing power, especially when

the area under study is wide, is a serious limitation in remote sensing problems. The Google Earth Engine (GEE) platform is a spatial processing platform for environmental monitoring and analysis. Very high speed, simultaneous processing, free access, support for programming languages such as Python and Java, support for most satellite data and no need for powerful hardware are among the most important advantages (Tamiminia et al., 2020). The development of GEE has created much enthusiasm and engagement in the remote sensing and geospatial data science fields (Tamiminia et al., 2020). Although this system has been developed since 2013, unfortunately, despite its many advantages, it has been used less in studies. Based on the estimates, remote sensing data has been used in 90% of studies, but only 10% of this information has used the ready data of this system (Tamiminia et al., 2020). Mansourmoghaddam et al. (2022) applied the GEE platform and MODIS satellite data to monitor and predict spatial and temporal changes of airborne dust during 6 years in Qazvin province, Iran. Evaluating relationships between vegetation cover changes and land degradation is very important. Desertification is one of the key issues of Iran's dry Sistan plain, which is located in the east (Shafiei and Hosseini, 2012). It is crucial to understand the causes and processes of desertification in order to regulate and stop it from progressing. Therefore, the goal of this study is to use the GEE platform and remote sensing techniques to track changes in the vegetation cover of a section of the Sistan Plain over a 10-year period (2011–2020) and investigation of the relationship between changes in vegetation with the amount of water used and rainfall. It is expected such results can implicitly indicate the amount of water withdrawal from underground water sources in the future researches.

2. Materials and methods

2.1. Study area

The Sistan plain is low-relief and Hirmand river delta that known as floodplain with significant wind erosion and sedimentation processes. This plain is situated in the province of Sistan and Baluchistan and including Hirmand, Hamon, Nimroz, Zahak, and Zabol counties. The study area's average elevation is 482 meters above sea level. The region's highest point, with a height of 500 meters, is found in the southern part of the plain, inside the boundaries of Zahak county. The lowest point, with a height of 467 meters, is situated in the Hamon region on the banks of the Sistan River near the entrance of the river to Hamon lake. The studied area with an area of 203 thousand hectares is located between longitude 61°18' to 61°52' E and latitude 30°50' to 31°20' N (Figure 1).

2.2. Collecting data

To prepare vegetation maps in different years (2011 to 2020), Landsat 8 satellite images (OLI sensor) with special resolution 30 m were used for the months of April to the end of October, when most of the agricultural activities in the Sistan plain are limited to these months (Firouzi et al., 2019). All pre-processing operations, satellite image processing and NDVI vegetation index calculations were performed using the GEE platform. In this research, the NDVI index was calculated for each year using the median filter in the GEE platform, and the NDVI index was calculated using the following relationship:

$$\mathrm{NDVI} = \frac{\mathrm{NIR}-\mathrm{RED}}{\mathrm{NIR}+\mathrm{RED}} \quad (1)$$

In this regard, NIR and RED indicate infrared and red bands, respectively. NDVI values vary from +1 to -1. Values close to +1 indicate vegetation, zero indicates land without vegetation (soil), and values close to -1 indicate moisture (Haku and Basak, 2017).

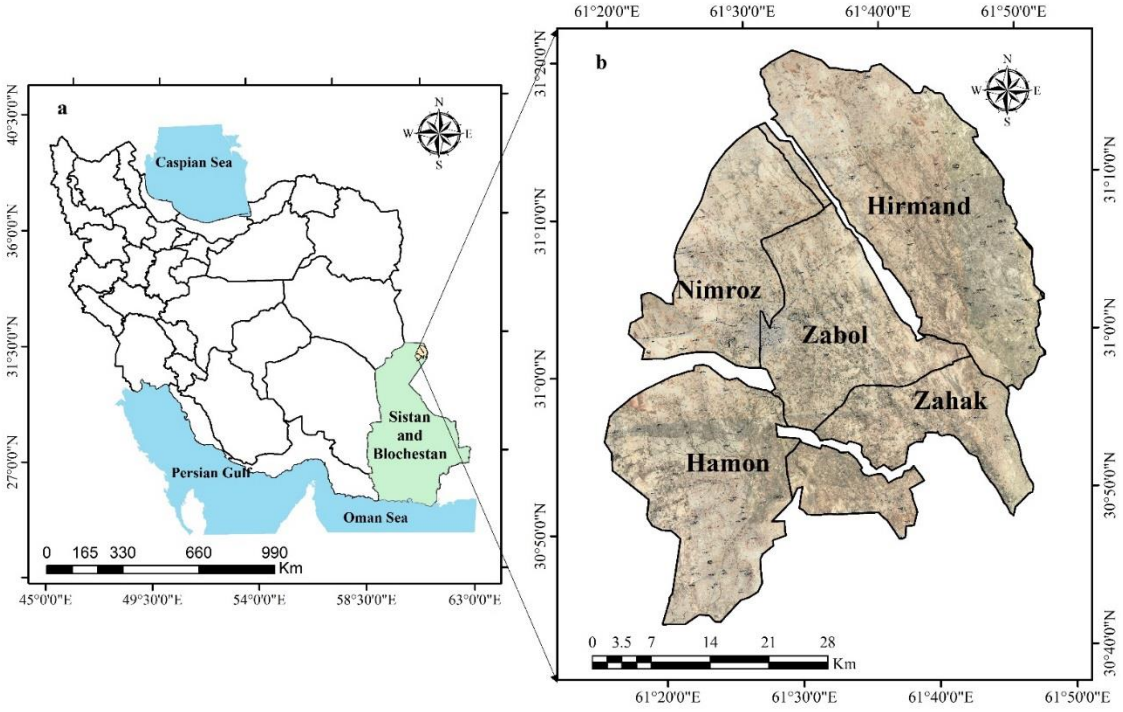

Fig. 1. The location of the study area in iran (a) and in counties of Sistan and Baluchistan Province (b)

2.3. Preparation of classified images

At this stage, utilizing the decision tree (DT) algorithm in accordance with the ENVI 5.3 software's definitions for this algorithm and the NDVI values. The NDVI values greater than 0.3 have vegetation and NDVI values equal to zero are equivalent to bare lands (Gandhi et al., 2015). The DT is one of the most intuitive classifiers with a set of decision-rules which convert inputs, such as measured spectral reflectance, into discrete thematic outputs, or classes (e.g. land cover and bare land classes in our case). Each pixel, with all its input information will be assigned to a land cover class based on the criteria defined in the decision-rules (i.e., the NDVI values). It has tree-like structure, which is organizes the decision-rules hierarchically and sequentially splits into the category. Each node contains a binary decision which evaluates an input to be either TRUE or FALSE. For a period of ten years, maps of the vegetation classification were created for two groups of lands with and without vegetation (crop and soil).

2.4. Validation of vegetation maps

By comparing the classified images with reference samples collected from ground supervised sampling, validation was carried out. Google Earth images from each year were utilized to identify the land points, and samples of plant and arid land were collected based on these images. The classified images were then tested using field data, and by creating an error matrix and calculating the overall accuracy indices (OA) and Kappa (K), the accuracy of the vegetation maps was assessed. The number of 60 points was taken into account in this study to assess the precision of the classification results. The following relationships were used to determine these indicators:

The fraction of the total samples that were correctly classified is shown by the map's overall accuracy, also known as general accuracy (OA). How many samples, in other words, are

accurately classified in the appropriate classifications? The classification's overall accuracy is an average that displays the proportion of correctly identified pixels to all known pixels. Several researchers used the OA and kappa coefficient to evaluate the accuracy of classification (Rwanga and Ndambuki, 2017; Mansourmoghaddam et al., 2022). By creating an error matrix and using the formula below, this feature can be calculated (Congalton, 1991):

$$OA = \sum_{i=1}^{n} X_{ii} / N \quad (2)$$

The Kappa coefficient is another index that is taken from the error matrix. The classification accuracy in comparison to a totally random classification is calculated using the kappa coefficient. This means that the Kappa value gives the classification accuracy compared to the case where an image is classified completely randomly. This work can be interpreted in such a way that after removing the influence of chance in the classification, the matching value with the ground reality will be calculated. One of the most famous estimates of Kappa using the elements of the error matrix is the equation (Congalton, 1991):

$$K = N\sum_{i=1}^{n} xX_{ii} - \sum_{i=1}^{n}(X_{io} \times X_{oi}) /N^2 - \sum_{i=1}^{n}(X_{io} - X_{oi}) \quad (3)$$

where n is the number of rows (and therefore columns) in the matrix, $X_{ii}$is the count in a diagonal cell where row and column i meet (i.e., correct classifications), Xio is the row total, Xoi is the column total, and N is the total number of observations.

2.5. Change detection analysis

After creating a map of the vegetation for the years 2011 to 2020, the vegetation changes were looked at for specific time periods, and a map of its changes was created, keeping in mind that the goal of this study is to analyze the process of vegetation changes. The theme change workflow approach were used to identify changes (Gondwe et al., 2021). This method produces a map of the vegetation change based on the classifications made using the decision tree algorithm for the two years in question. Three categories of changes—a reduction in vegetation, an increase in vegetation, and no changes—were taken into account when creating the map of vegetation changes.

3. Results and discussion

The vegetative area in 2011 equaled 29156.1 ha, while in 2012 it equaled 9537.9 ha. In 2011, the majority of the Sistan plain has a comparatively good vegetation cover, with the exception of the northern parts of the region, which are devoid of vegetation (Figure 2). In 2012, however, despite the fact that the region's overall vegetation cover has decreased significantly (19618.1 ha, or 67% less vegetation), this reduction is particularly pronounced in the northern and eastern parts of the region (primarily Hirmand county), which are now almost completely devoid of vegetation. Although the yearly rainfall in the area's synoptic stations, which include Zahak and Zabol stations, was marginally lower in 2011 than in 2012, the amount of incoming water from the Hirmand river increased in 2012 (Figure 3). As a result, in 2012 the region's river water supply decreased (Figure 4), which had an impact on agriculture and led to less cultivation this year. Firouzi et al. (2019) explained that in the Sistan plain, vegetation cover does not rely on rain but on the water flowing of the Hirmand River. Shafei and Hosseini (2012) using satellite data, examined the state of the vegetation in the Sistan region and assessed changes to the vegetation between 1990 and 2006. According to the findings, there was 26 thousand hectares of vegetation in 2006, down from 101 thousand hectares in 1990.

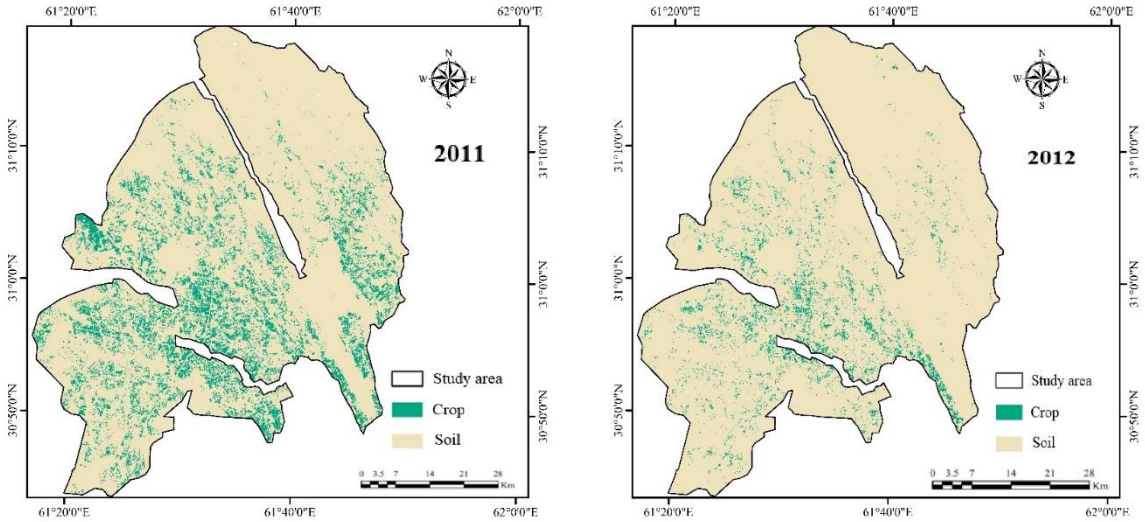

Fig. 2. Vegetation status of Sistan plain in 2011 and 2012

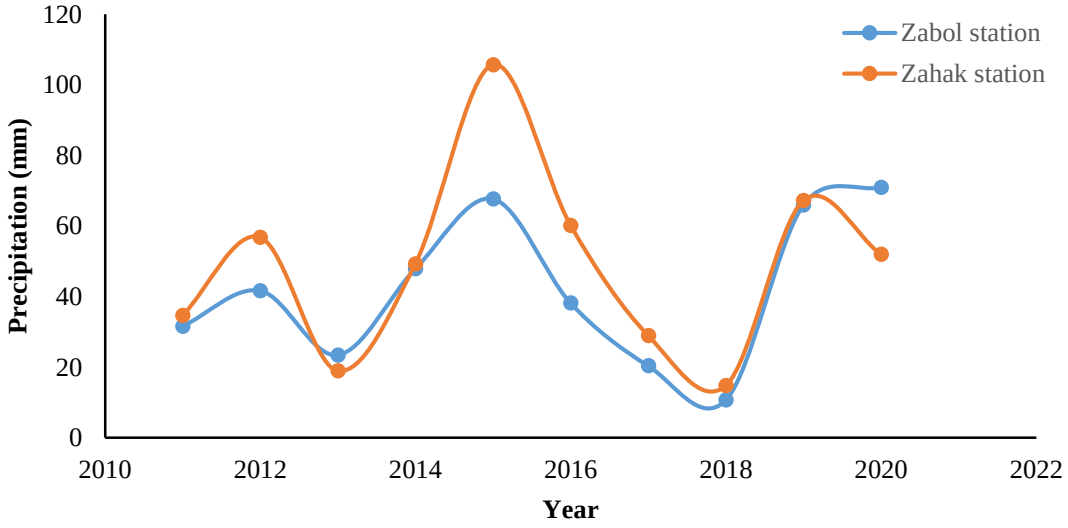

Fig. 3. The annual rainfall of Zabol and Zahak synoptic stations during the 2011 to 2020.

According to the maps that were collected in 2013 and 2014 (Figure 5), the area of vegetation in Sistan plain increased by 82.5% (or 3088.5 ha) between 2013 and 2014, reaching 6831.1 ha. It can be related to the increase in precipitation and Hirmand River's water level at this year. On the other hand, the findings indicate that the area of vegetation has increased, going from 31646.6 ha in 2015 to 30201.8 ha in 2016, with a drop of 4.6 percent (Figure 6).

The Sistan plain's vegetation state in 2017 and 2018 are shown in Figure 7. According to the maps that are now accessible, the amount of vegetation in 2017 was equal to 31103.0 ha, and it decreased significantly in 2018 to reach 17834.6 ha (i.e., 42.6% decline or 13268.4 ha). It should be noted that variations in the Sistan plain's vegetation are significantly influenced by

the Hirmand River's water level. The Hirmand River's flow is constantly changing (Figure 4), thus in addition to providing drinking water, it has also seriously harmed the ecosystem in years when there have been droughts and water shortages. In some years, floods have also been associated with the river's flow. Drought conditions and a decrease in water flow from Hirmand's sources have led to a catastrophe in this region and a reduction in water flow towards Sistan (Sharifikia, 2013). Because of the Sistan plain's low levels of precipitation, high levels of evaporation- transpiration, the Hirmand River serves as a major source of water for this area, and its hydrological variations have changed the vegetation.

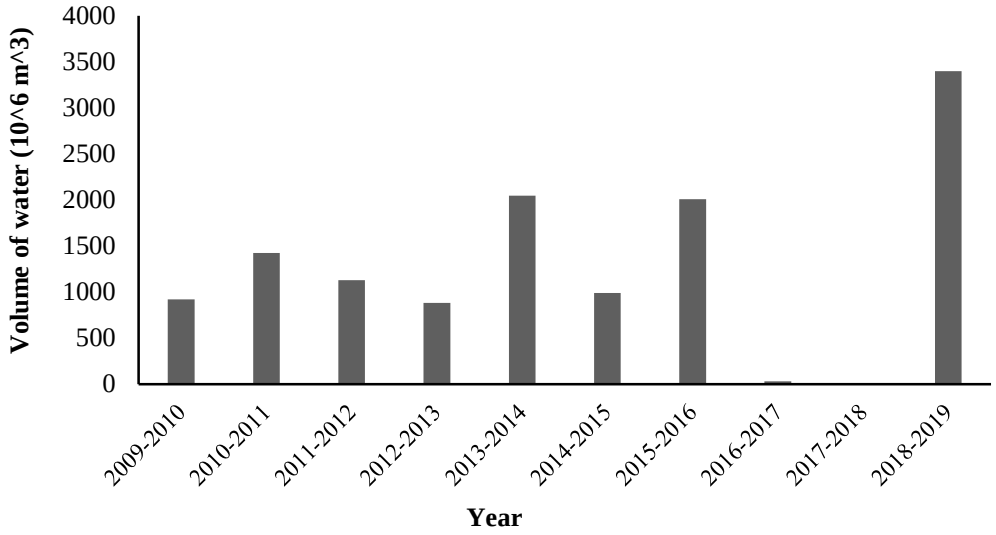

Fig. 4. Hirmand river water inflow to Sistan region in different years.

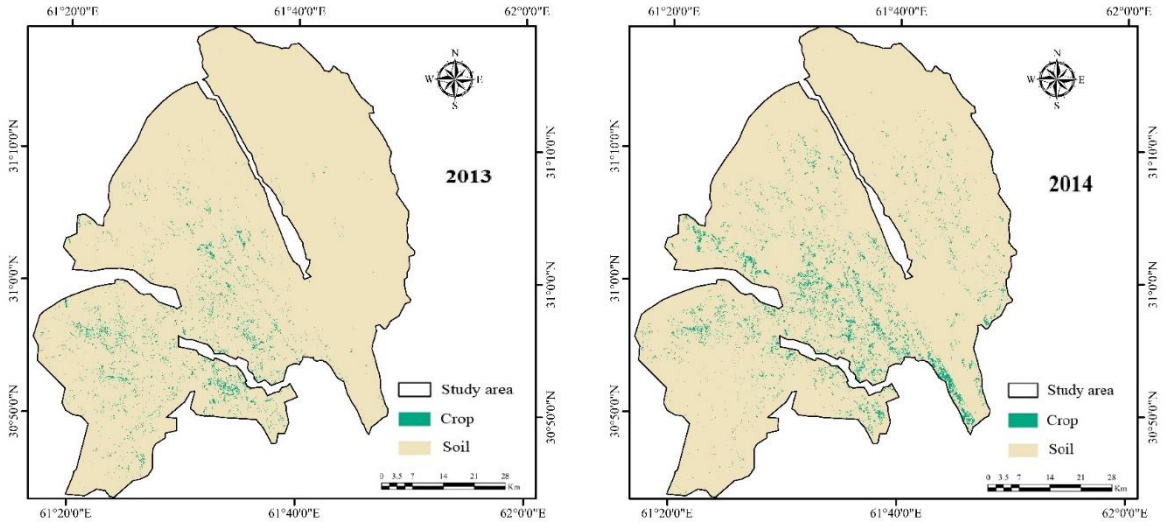

Fig. 5. Vegetation status of Sistan Plain in 2013 and 2014.

The Sistan Plain's vegetation cover has improved during the past two years (2019 and 2020), and as a result, in 2019 there was a 4.5% increase in vegetation compared to 2018. It has reached

37464.0 ha (Figure 8). Examining the volume of incoming water from the Hirmand river as well as the amount of rainfall over the past two years (2019 and 2020) reveals that, in addition to an increase in rainfall, the volume of water in the Hirmand River has also increased significantly, which has contributed to the success of agriculture in this area. Additionally, it should be emphasized that the vegetation in this area depends heavily on the amount of water from the Hirmand River and its arrival, and that an increase in rainfall cannot significantly affect the changes in vegetation due to the high rates of evaporation - transpiration in this location.

In order to look into the vegetation changes on Qeshm Island between 2001 and 2014, Nateghi et al. (2018) assessed four vegetation indices, including NDVI, SAVI, RVI, and WAVI. The findings showed that inside the island, agricultural areas and natural vegetation had increased by 60% and the size of mangrove forests by 21% during the past 13 years, respectively.

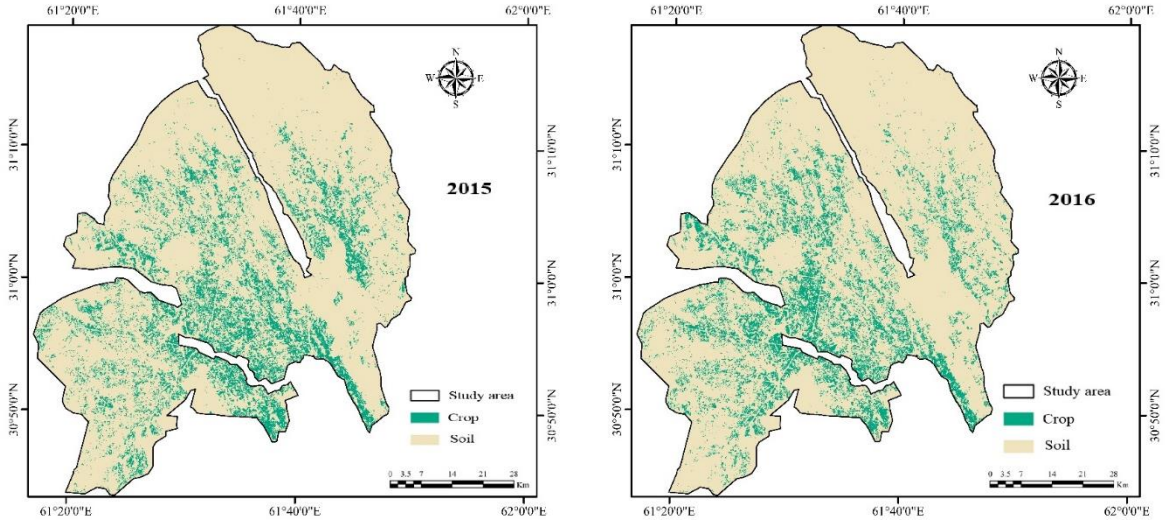

Fig. 6. Vegetation status of Sistan Plain in 2015 and 2016

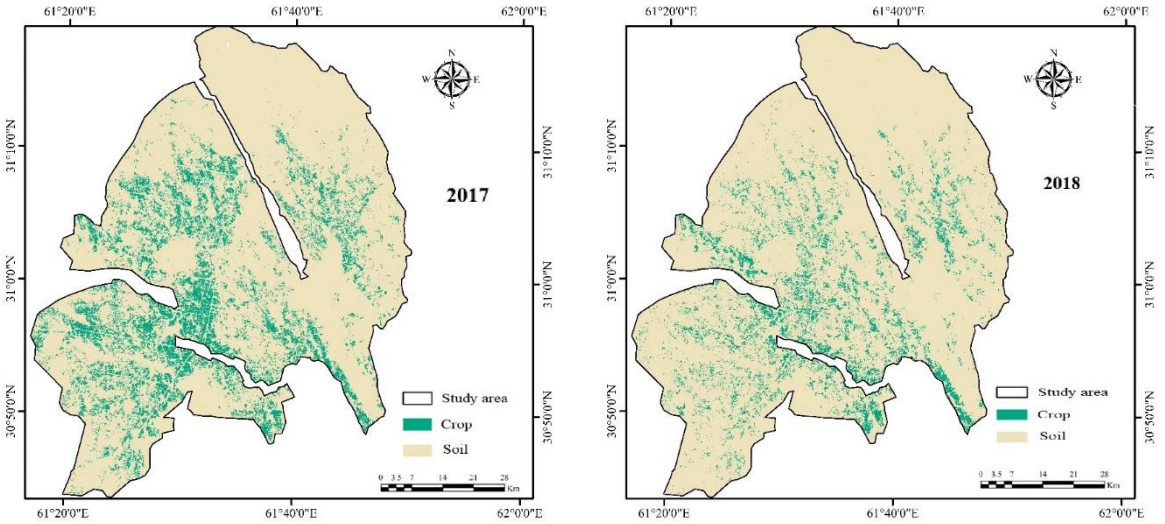

Fig. 7. Vegetation status of Sistan Plain in 2017 and 2018.

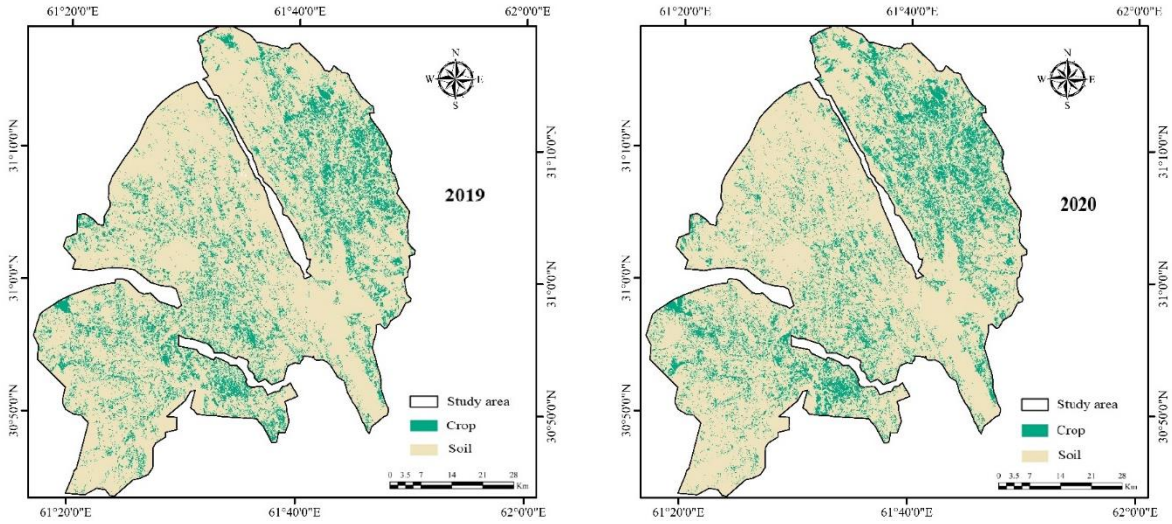

Fig. 8. Vegetation status of Sistan Plain in 2019 and 2020.

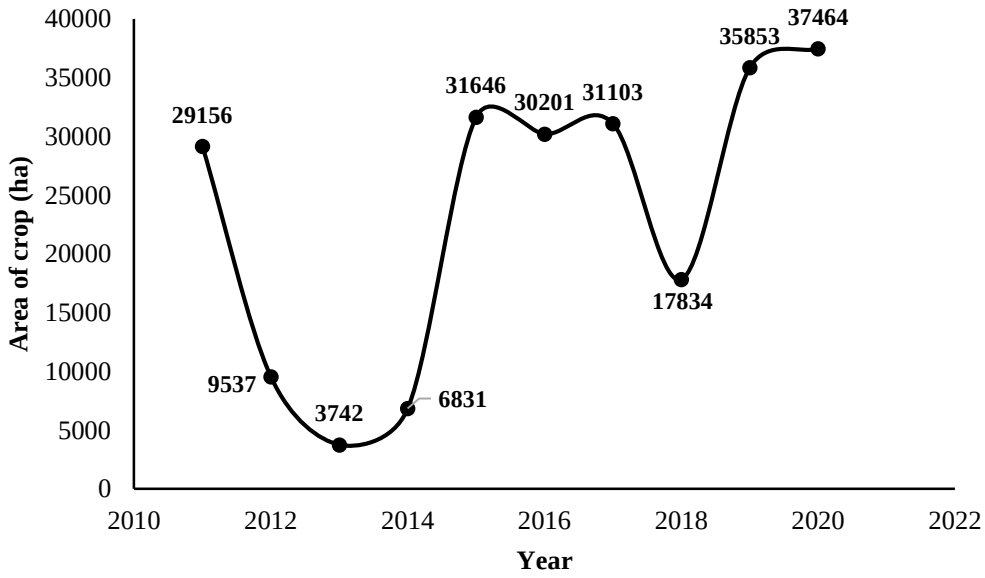

Fig. 9. Vegetation changes trend in Sistan plain during 10 years.

The overall pattern of vegetation changes over a ten-year period in the Sistan plain is shown in Figure 9. Based on this, the study area has the worst vegetative conditions during the years 2012 to 2014. After that, there is an increase in vegetation with a fairly steep slope, and after two years of stability, there is a subsequent reduction in vegetation (Figure 9). Tables 1 and 2 indicate an example of the error matrix for 2013 year, and validation outcomes of NDVI classified maps for various years, respectively. The overall accuracy and kappa values show where the NDVI classified maps are most accurate. Kappa values more than 0.8, 0.8 to 0.4, and less than 0.4, respectively, according to Congalton and Green (1998), imply strong, moderate, and low agreement between the projected values. Thus, it can be concluded from the Kappa values that there is a moderate agreement between the ground samples and the classified images.

Table 1. Error matrix comparing actual samples and classified images for 2013 year

		Actual condition		Total
		Crop	Soil	
Classified images	Crop	19	0	19
	Soil	10	31	41
Total		29	31	60

Table 2. Validation results of NDVI classified maps in different years

Year	Overall accuracy (%)	Kappa index
2011	84.4	0.68
2012	73.3	0.47
2013	83.0	0.66
2014	74.0	0.49
2015	85.0	0.7
2016	85.0	0.7

Utilizing the detection method has the benefit of allowing you to keep track of these changes (Mousavi et al., 2017). These changes have been generated in the form of a map utilizing detection analysis and divided into three groups: decline in vegetation, increase in vegetation, and no changes in order to better understand the process of vegetation changes. Fig. 10 shows the variations in the Sistan plain's vegetation between 2012 and 2011. In this time, 19443.6, 1320.1 and 182519.2 ha of land show decline, increase and o change in vegetation cover (Table 3). Fig. 11 displays the vegetation change map of the Sistan plain in 2015 compared 2014. According to this results, the Sistan plain as a whole has experienced the trend of growing vegetation cover, with 24055.0 ha of vegetation cover increasing, 681.0 ha of vegetation cover decreasing, and 178697.2 ha remaining unchanged (Table 3).

In comparison to 2015, Fig. 12 depicts the vegetation of the Sistan plain in 2018. This map shows that vegetation has grown and decreased throughout the entire region, with no discernible trend. In this period of time, 16111.9 ha of vegetation cover decreased, 3234.4 ha of vegetation cover increased and 184090.2 ha remained unchanged (Table 3). Fig. 13 displays the Sistan plain's vegetation changes between 2020 and 2018. Vegetation decreased on 10006.7 ha of land, grew on 27934.5 ha, and not changed in 165370.2 ha (Table 3). Fig. 14 depicts the modifications to the Sistan plain's vegetation from 2020 to 2011. According to this map, the Sistan plain's middle regions have experienced a reduction in vegetation, while the region's northern and eastern regions (i.e., particularly Hirmand county) have seen an increase. Generally, throughout the ten years (2011 to 2020) in Sistan plain, vegetation cover declined on 19260.4 ha of land and increased in 25633.2 ha of land (Table 3). Due to the disruption of the water supply, the drying up of lakes, and the consequent abandonment of agricultural fields, droughts play a significant part in the loss of vegetation. The most significant causes of the decline in vegetation in this area have generally been the drought, the complete drying of Hamun Lake and the lack of access to alternative water sources, such as the absence of alternative underground water sources or alternative surface water sources. The comparison of the categorized photos revealed that the agricultural lands that were not cultivated and left fallow during the drought are what are mostly responsible for the decline in vegetation. The remaining portion of the loss in vegetation cover is

attributed to grazing areas, riverbanks, and reeds that were already present in the study area.

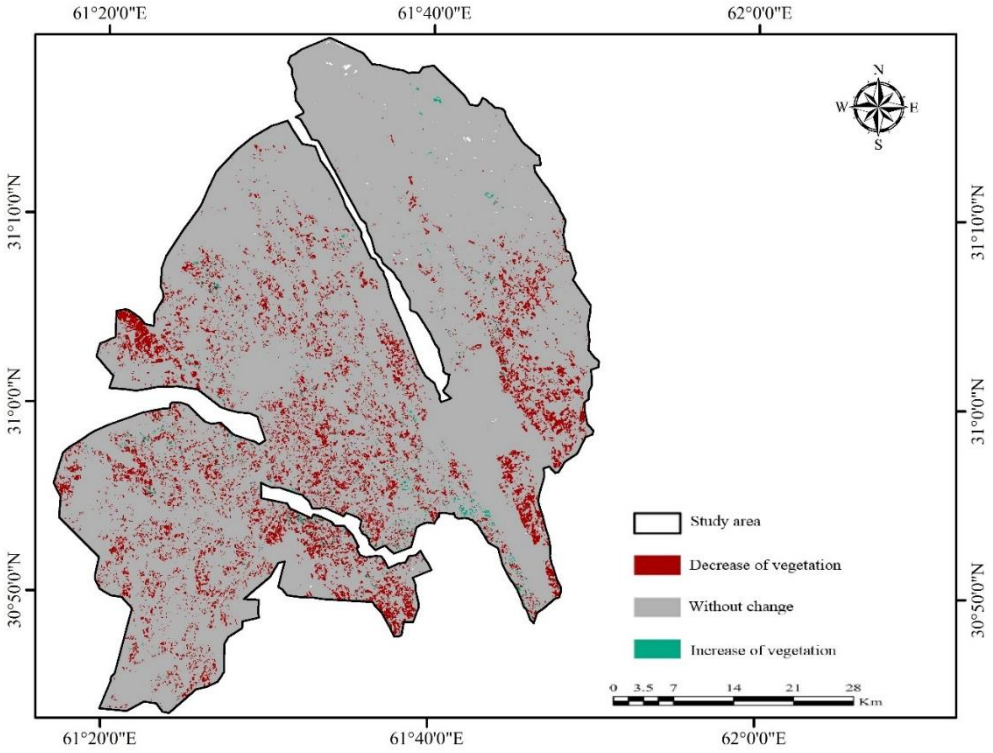

Fig. 10. Vegetation changes in Sistan plain in 2012 compared to 2011.

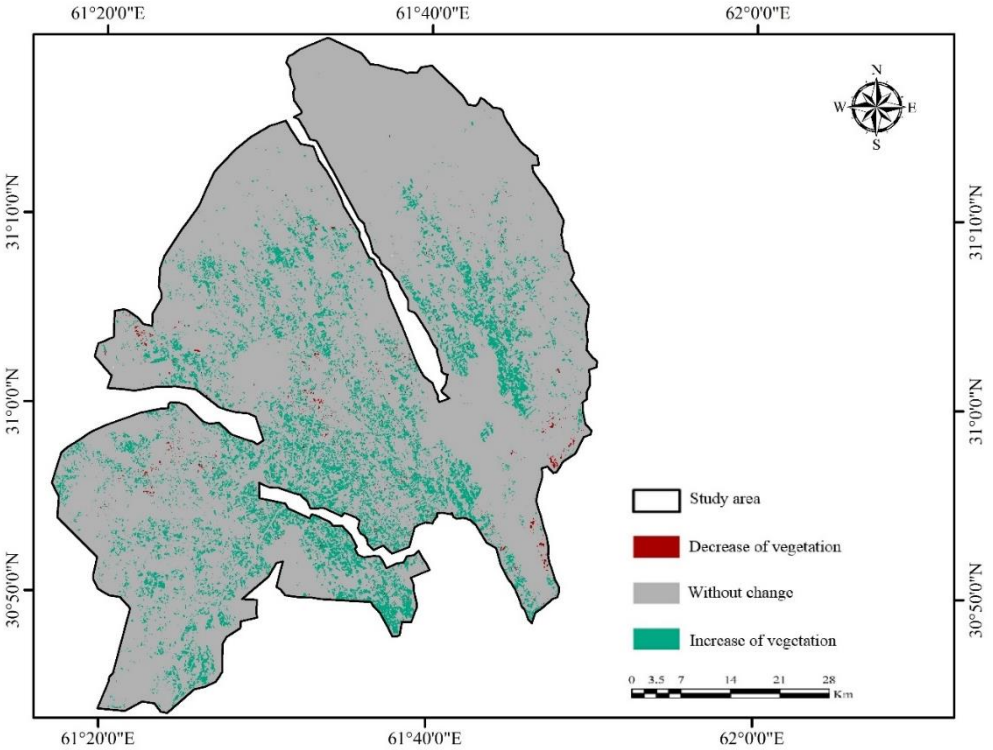

Fig. 11. Vegetation changes in Sistan plain in 2015 compared to 2014.

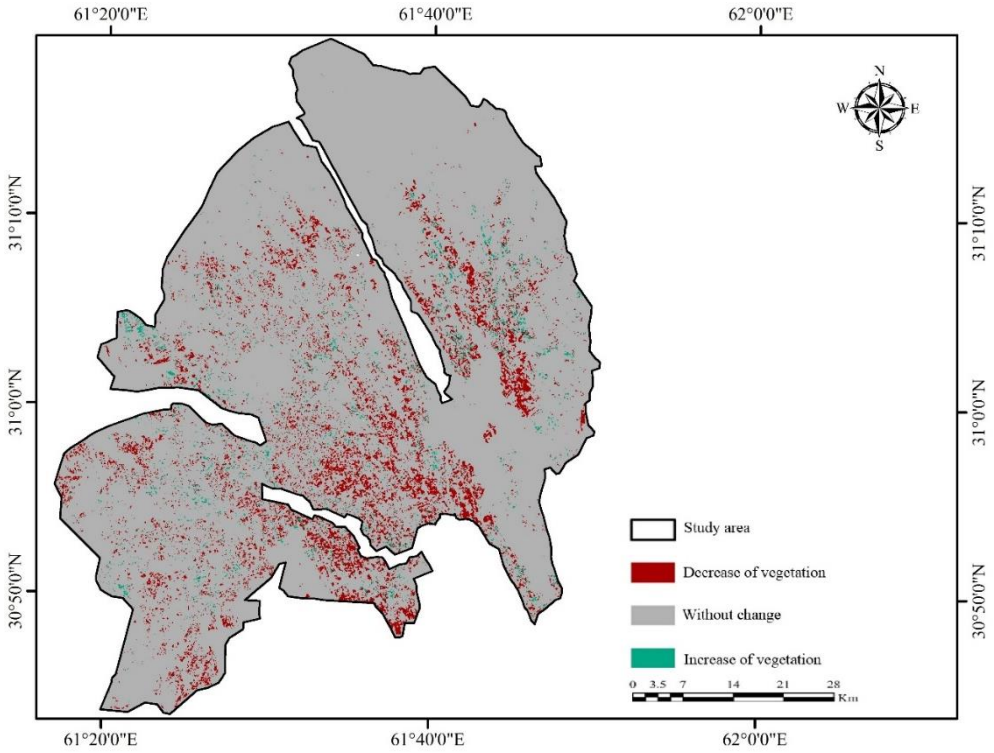

Fig. 12. Vegetation changes in Sistan plain in 2018 compared to 2015.

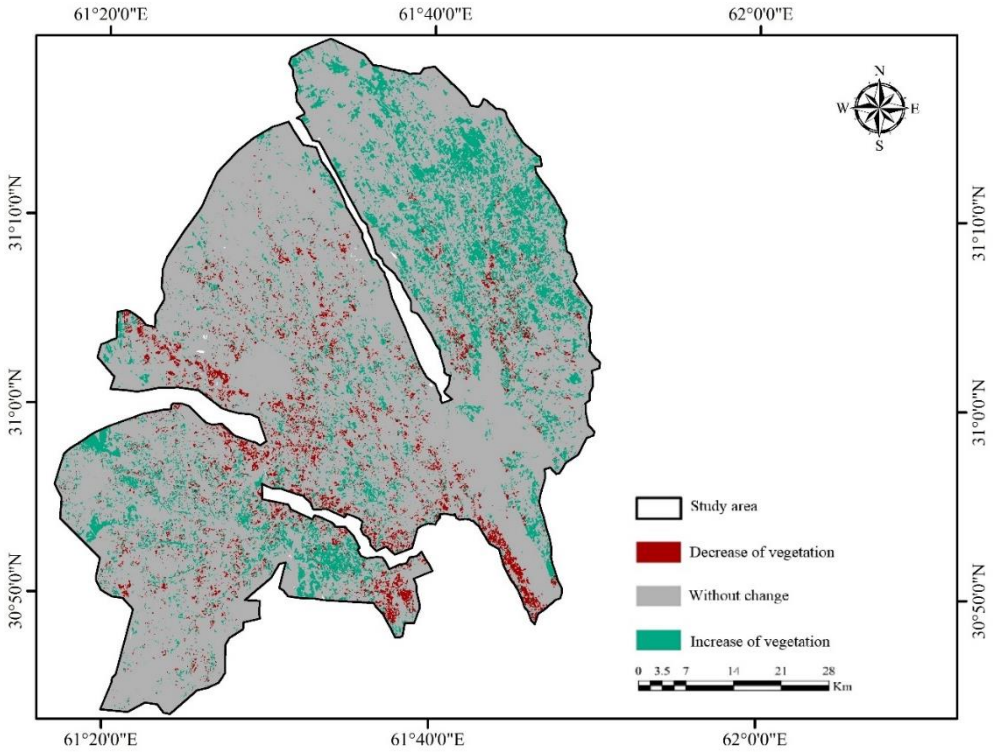

Fig. 13. Vegetation changes in Sistan Plain in 2020 compared to 2018

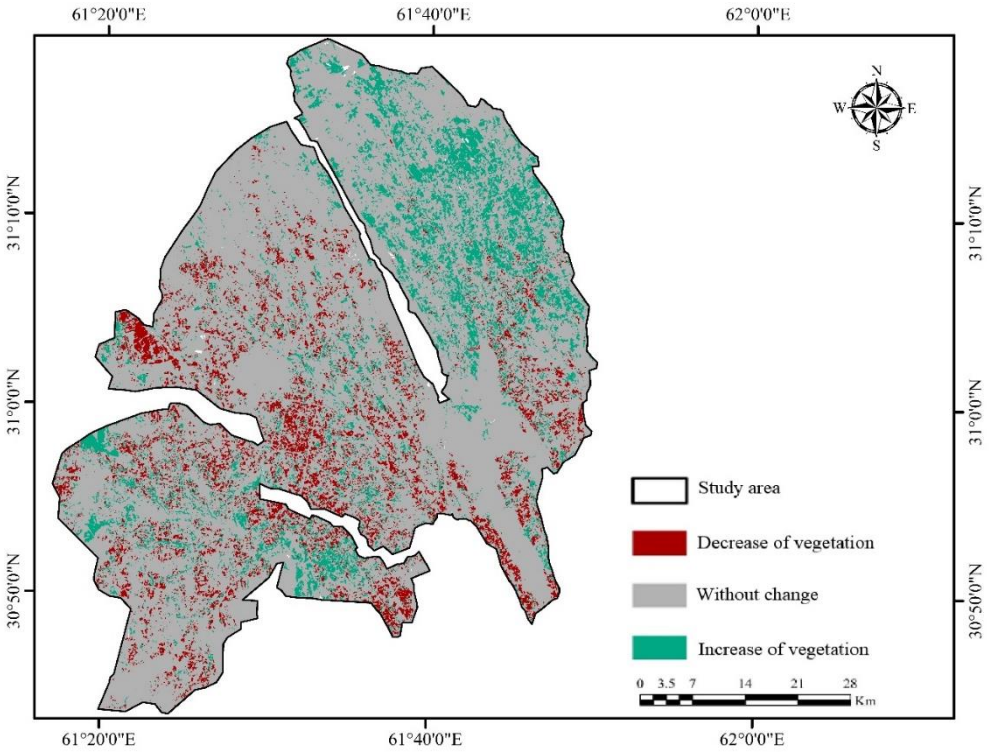

Fig. 14. Vegetation changes in Sistan Plain in 2020 compared to 2011.

Table 3. The area of vegetation changes in different time periods based on the analysis of the detection of changes

Times	Decrease of vegetation (ha)	Increase of vegetation (ha)	Without change (ha)
2011-2012	19443.6	1320.1	182519.2
2014-2015	681.0	24055.0	178697.2
2015-2018	16111.9	3234.4	184090.2
2018-2020	10006.7	27934.5	165370.2
2011-2020	19260.4	25633.2	158272.3

4. Conclusion

Utilizing remote sensing technology, the current study tracked agricultural vegetation changes in the Sistan plain over a period of ten years (2011 to 2020). The findings indicate that the study area's vegetation was at its poorest from 2011 to 2014. It should be noted that variations in the Sistan plain's vegetation are significantly influenced by the Hirmand River's water level. The Hirmand river's flow has always fluctuated, so in addition to supplying drinking water in some years and causing severe environmental harm in others owing to drought and water scarcity, it has also occasionally been accompanied by floods. The Sistan plain's agricultural area has decreased due to a lack of rainfall, high rates of evaporation-transpiration, unpredictability in Hirmand River's flow rate, and a general lack of available water resources in the area. Drought conditions and reduced water flow from Hirmand's sources have resulted in decreased water flow toward Sistan and the development of a catastrophe in this region. Because of the Sistan plain's low levels of precipitation, high levels of evaporation-transpiration, the Hirmand River

serves as a major source of water for this area, and its hydrological variations have changed the vegetation there. Making management decisions and comprehending environmental changes are facilitated by knowing the process of vegetation change. As a result, the findings of this study enable management choices for regional planning. It is advised to employ satellite photos with high spatial resolution to reveal more precise changes for better and more accurate monitoring of vegetation changes.

References

Alavipanah, S.K., 2003. Application of remote sensing in earth science. 5th ed., University of Tehran Press, Tehran.

Alavipanah, S.K., Ehsani, E., Metinfar, H., Rafii Imam, A., Amiri R., 2006. Comparison of information content of TM and ETM+ sensor bands in desert and urban environments of Iran. Journal of Geographical Studies. 47; 56-64.

Alqurashi, A.F., Kumar, L., 2013. Investigating the use of remote sensing and GIS tech- niques to detect land use and land cover change: a review. Advances in Remote Sensing. 2; 193–204.

Braun, A., Fakhri, F., Hochschild, V., 2019. Refugee camp monitoring and environmental change assessment of Kutupalong, Bangladesh, based on radar imagery of Sentinel-1 and ALOS-2. Remote Sensing.11; 1–34.

Congalton, R. 1991. A review of assessing the accuracy of classifications of remotely sensed data. Remote Sensing Environmental 37: 35–46.

Congalton, R.G., and Green, K., 1998. Assessing the Accuracy of Remotely Sensed Data: Principles and Practices. CRC Press, Boca Raton.

Fatemi, S.B., Rezaie Y. 2012. Basics of remote sensing. Azadeh. Iran.

Firouzi, F., Tavossi, T., Mahmoudi, P. 2019. Investigating the sensitivity of two vegetation indices, NDVI and EVI, to droughts and droughts in arid and semi-arid regions; Case study: Sistan plain of Iran. Scientific - Research Quarterly of Geographical Data (SEPEHR). 28, 163- 179.

Gandhi, M., Parthiban, S., Thummalu, N., Christy, A., 2015. Ndvi: Vegetation change detection using remote sensing and GIS – A case study of Vellore District. Procedia Computer Science 57, 1199 – 1210.

Gondwe, J.F., Lin, S., Munthali, R.M., 2021. Analysis of Land Use and Land Cover Changes in Urban Areas Using Remote Sensing: Case of Blantyre City. Discrete Dynamics in Nature and Society. 2021, 1-17.

Kotaridis, I., Lazaridou, M., 2018. Environmental change detection study in the wider area of lignite mines. Civil Engineering and Architecture. 6; 108–114.

Lu, D., Mausel, P., Brondízio, E., Moran, E., 2004. Change detection techniques. International Journal of Remote Sensing. 25; 2365-2407.

Mohammadyari, F., Mirsanjari, M.M., Zarandian, A., 2019. Monitoring of vegetation changes in Karaj watershed using NDVI index and gradient analysis. Journal of RS and GIS for Natural Resource. 4; 55-72.

Mansourmoghaddam, M., Ghafarian Ghafarian Malamiri, Arabi Aliabad, F., Fallah Tafti, M., Haghani, M., H.R., Shojaei, S. 2022. The Separation of the Unpaved Roads and Prioritization of Paving These Roads Using UAV Images. Air, Soil and Water Research. 15.

Mansourmoghaddam, M., Naghipur, N., Rousta, I., Ghaffarian, H.R. 2022. Temporal and Spatial Monitoring and Forecasting of Suspended Dust Using Google Earth Engine and Remote Sensing Data (Case Study: Qazvin Province). Desert Management. 10; 77-98.

Mousavi, M.N., Sarli, R., Khodadad, M. 2017. Revealing changes in land use and vegetation in Poldakhter city using Landsat satellite images. Environmental studies of Haft Hesar. 26; 103-115.

Nateghi, S., Nohegar, A., Ehsani, A.H., Bazrafshan, O., 2018. Evaluating the vegetation changes upon vegetation index by using remote sensing. Iranian Journal of Rangeland and Desert Research. 4; 778-790.

Pettorelli, N.,Vik, O., Mysterud. A., Gaillard, J. M,. Tucker, C. J. and Stenseth.N. C., 2005. Using the satellite–derived NDVI to assess ecological responses to environmental change. Journal Trends in Ecology and Evolution. 9; 200-216.

Rahman, M., Islam, M., Chowdhury, T., 2019. Change of vegetation cover at Rohingya refugee occupied areas in Cox's Bazar District of Bangladesh: evidence from remotely sensed data. Journal of Environmental Science and Natural Resources. 11; 9–16.

Reynolds, J. F.; D.M. Smith, E.F. Lambin, B.L. Turner, M. Mortimore, S.P. Batterbury, T. E.Downing, H. Dowlatabadi, R.J. Fernandez, J.E. Herrick, E. Huber-Sannwald, H. Jiang, R. Leemans, T. Lynam, F.T. Maestre, M. Ayarza, and B. Walker. 2007. Global desertification: building a science for dryland development. Science. 316; 847-851.

Rwanga, S.S., Ndambuki, J.M. 2017. Accuracy assessment of land use/land cover classification using remote sensing and GIS. International Journal of Geosciences. 8, 1-12.

Shafei, H., Hosseini, S. M., 2012. A study of vegetation in Sistan region through satellite data. Journal of Plant Ecophysiology. 9; 91-105.

Tamiminia, H., Salehi, B., Mahdianpari, M., Quackenbush, L., Adeli, S., Brisco, B., 2020. Google Earth Engine for geo-big data applications: A meta-analysis and systematic review. ISPRS Journal of Photogrammetry and Remote Sensing. 164; 152–170.

Veron, S.R., Paruelo, J.M., Oesterheld, M., 2006. Assessing desertification. Journal of Arid Environments. 66; 753-763.

Xie, Z., Phinn, S.R., Game, E.T., Pannell, D.J., Hobbs, R.J., Briggs, P.R., McDonald-Madden, E. 2019. Using Landsat observations (1988–2017) and Google Earth Engine to detect vegetation cover changes in rangelands - A first step towards identifying degraded lands for conservation. Remote Sensing of Environment. 232; 111317.